EVIDENCE OF NORMAL FAULTING OF THE OUTER RINGS OF ORIENTALE BASIN: PRELIMINARY MODELING RESULTS. Amanda L. Nahm[1,2] and David A. Kring[1,2], [1]USRA-Lunar and Planetary Institute, 3600 Bay Area Blvd., Houston, TX 77058, USA, [2]NASA Lunar Science Institute.

Introduction: The lunar Orientale basin, with a crater-rim diameter in excess of 900 km, is the best-preserved and youngest multi-ring basin on the Moon [1–5]. It is located on the Moon's western limb [1, 6] in the lunar highlands [6] and is centered at approximately 20ºS, 265ºE. Orientale basin consists of at least four concentric rings [4] (Fig. 1). The outermost ring, called the Cordillera ring, defines the extent of the basin [2]. The interior ring structures, the Inner Rook and Outer Rook rings, have diameters of 480 km and 620 km, respectively [2, 4]. An inner ring with a diameter of about 320 km surrounds a flat, low albedo unit that appears to partially fill the center of the Orientale basin and is known as Mare Orientale [1, 2]. The cratering processes that produce multi-ring basins remain unknown and their resolution is one of the science priorities targeted by the National Research Council [7].

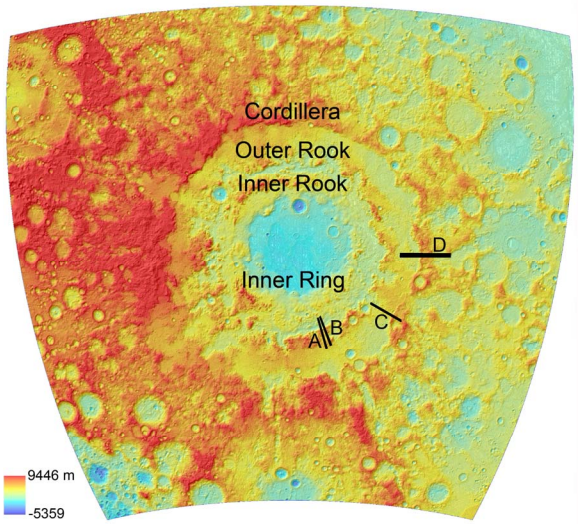

Fig. 1. LRO LOLA topography for Orientale Basin with locations of topographic profile sets shown and rings labeled for reference. Elevation scale is shown at lower left in meters above or below the lunar reference datum. North is up. Resolution: 256 px/deg. Orthographic projection centered at 20°S, 263.75°E.

Here, we test hypotheses for the formation of the Cordillera and Outer Rook rings using detailed topographic analysis and forward mechanical modeling of the ring scarps. Several mechanisms have been proposed for the formation of these rings in Orientale and other lunar multi-ring basins. In some cases, the models predict normal faulting at the Outer Rook and Cordillera rings [e.g., 5, 8–13], while others do not.

Methods: To test the diverse models of basin formation, we use the forward mechanical dislocation modeling program Coulomb (available from http://earthquake.usgs.gov/research/modeling/coulomb/overview.php) [14, 15] to model surface displacements associated with normal faulting, which are then compared to measured LOLA topographic profiles across the rings. Forward mechanical modeling has been used successfully to model the surface displacements of faults on Mercury [16], Earth [e.g., 17–21], and Mars [e.g., 22–25]. This is the first application of the method to impact structures and to faults on the Moon.

In our models, a fault surface is idealized as a rectangular plane, with the sense of slip (i.e., normal, thrust, strike-slip, or oblique), magnitude of displacement, fault dip angle, depth of faulting, and fault length specified, and material displacements are calculated [26]. Model parameters are determined based on the fit between observed (measured LOLA) and predicted (modeled) topography [16] of the footwall flexural uplift. The initial displacement magnitude is estimated from the relief of the scarp (here, ~3 km) and adjusted based on model output. A Young's modulus E of 100 GPa and Poisson's ratio v of 0.25 are assumed for the anorthositic rock mass for the pre-impact surface [27–29].

Topographic profiles were derived from gridded LOLA topography in the locations shown in Fig. 1. Each lettered heavy line denotes the location of several topographic profiles. These individual profiles were stacked to create average profiles. Profiles A and D are shown in Figure 2 as heavy black lines. Profile A is an average of 4 profiles and D is an average of 8 profiles spaced approximately 1.5 km and 1.8 km apart, respectively.

Results: Here, we present the first modeling evidence of normal faulting of the outer rings of Orientale basin. Figure 2 illustrates the fit of the calculated material displacements of several models to the LOLA topographic profiles. In profile A, the model shows that two parallel normal faults are intersected. Generally, the models that best fit the master fault (labeled 1 in Fig. 2) have faults that dip to the northwest toward the center of the basin at 70°, displacements of 4.5 km, and depths of faulting of 30–40 km. The models for the secondary fault (labeled 2 in Fig. 2) have faults that dip northwest at 60°, displacements of 1.45 km, and depths of faulting between 20 and 40 km (Table 1). Similar values for best fit parameters are found for the single fault transected by profile D. Broadly, the model normal faults dip 70° to the west, have displacements of 4.5–5 km, and

depths of faulting of 30–35 km (Table 1). According to a recent estimate, the average crustal thickness in this area is about twice this depth, ~60 km [30].

Since the models of displacements by planar, rectangular normal faults match the LOLA profiles well, these results also imply that the normal faults that formed the outer rings on the eastern side of the basin are planar and not listric at depth as is assumed by several models [e.g., 8, 11, 13], although this was not tested explicitly.

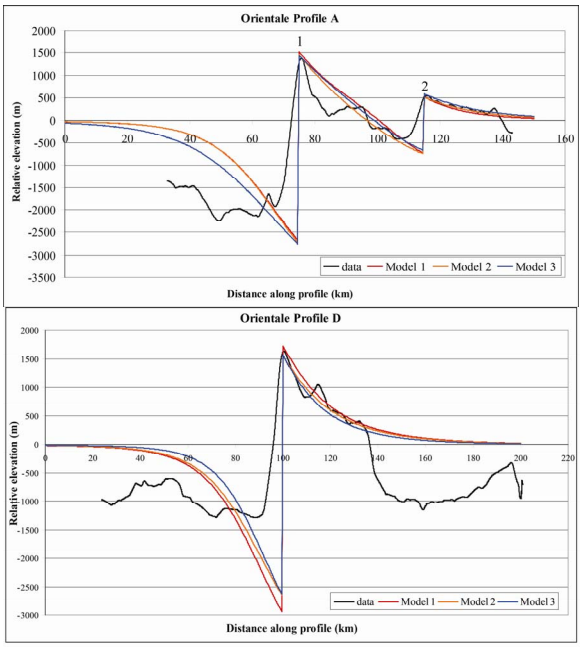

Fig. 2. Modeling results and averaged LRO LOLA topographic profiles derived from gridded LOLA topography for profiles A and D. Locations of profile sets shown in Fig. 1. Bold lines: average profile. Colored lines: Coulomb model results. See Table 1 for model parameters. The interior of the basin is to the left in both profiles. Average profile A (VE 15:1) transects the Outer Rook ring and average profile D (VE 23:1) transects the Cordillera ring.

Table 1. Fault parameters for the models shown in Fig. 2. Parameters listed in order (left to right) of Model 1 (red), 2 (orange), and 3 (blue).

Profile A		
	Fault 1	***Fault 2***
Dip angle (°)	70, 70, 70	60, 60, 60
Displacement (km)	4.5, 4.5, 4.5	1.45, 1.45, 1.45
Fault depth (km)	30, 30, 40	20, 30, 40
Profile D		
Dip angle	70, 70, 70	-
Displacement (km)	5, 4.5, 4.5	-
Fault depth (km)	35, 35, 30	-

In contrast, topographic profiles and images of the Inner Ring suggest that this ring formed in a manner different than the outer two rings of Orientale basin, perhaps from the collapse of a central peak to form a peak ring [31].

Conclusions: These results suggest the Cordillera and Outer Rook rings were produced by collapse of basin walls towards the basin center along planar normal faults, rather than along thrust faults or listric normal faults. These results are consistent with observations at the Chicxulub impact crater, which is the best terrestrial analog for basin-forming events. At Chicxulub, seismic data show vertical offset of stratigraphy of ~3–6 km along normal faults forming the structure's rim and an inner ring [31].

Our model results also illustrate that forward mechanical modeling is applicable to impact basins on the Moon and is useful for determining the locations and important parameters (dip angle, displacement magnitude and sense, and fault depth) of ring-forming faults, which can be used to understand basin- and ring-formation.

References: [1] Hartmann, W. K. and G. P. Kuiper (1962), Univ. of Az. LPL Comm., 1, 51–66. [2] Head, J. W. (1974), *The Moon 11*, 327–356. [3] Moore, H. J., et al. (1974), *PLSC* 5th, 71–100. [4] McCauley, J. F. (1977), *Phys. Earth Planet. Int. 15*, 220–250. [5] Spudis, P. D. (1993), *The Geology of Multi-ring Impact Basins*, Cambridge Univ. Press, 263 pp. [6] Spudis, P. D., et al. (1984), *JGR 89*, C197–C210. [7] National Research Council Report (2007), National Academies Press, 120 pp.[8] Mackin, J. H. (1969), *GSA Bull. 80*, 735–747. [9] Hartmann, W. K. and Yale, F. G. (1968), Univ. of Az. LPL Comm. *7*, 131–137. [10] Head, J. W. (1977), *in* Roddy, D. J., et al., eds., 563–573. [11] Head, J. W. et al. (1993), *JGR 98*, 17149–17181.[12] Melosh, H. J. and McKinnon, W. B. (1978), *GRL 5*, 985–988. [13] Head, J. W. (2010), *GRL 37*, L02203. [14] Lin, J. and Stein, R. S. (2004) *JGR 109*, B02303. [15] Toda, S., et al. (2005) *JGR 110*, B05S16. [16] Watters, T. R., et al. (2002) *GRL 29*. [17] King, G. C. P., et al. (1988), *JGR 93*, 13307–13318. [18] Toda, S., et al. (1998) *JGR 103*, 24543–24565. [19] Cohen, S. C. (1999) *Adv. Geophys*. *41*, 133–231. [20] Muller, J. R. and Aydin, A. (2005) *JGR 110*, B03407. [21] Resor, P. G., *GSA Bull. 120*, 414–430. [22] Schultz, R. A. (2000) *JGR 105*, 12035–12052. [23] Schultz, R. A. and Lin, J. (2001) *JGR 106*, 16549–16566. [24] Schultz, R. A. and Watters, T. R. (2001) *GRL 28*, 4659–4662. [25] Grott, M., et al. (2007) *Icarus 186*, 517–526. [26] Okada, Y. (1992) *Bull. Seismol. Soc. Am. 82*, 1018–1040. [27] Schultz, R. A. (1995), *Rock Mech. Rock Eng. 28*, 1–15. [28] Schultz, R. A. (1996), *JSG 18*, 1139–1149. [29] Turcotte, D. L. and Schubert, G. (2001), *Geodynamics*, Cambridge Univ. Press, 458 pp. [30] Ishihara, Y. et al. (2009) *GRL 36*, L19202. [31] Morgan, J. and Warner, M. (1999) *Geology 27*, 407–410.

Acknowledgements: We thank Brian Fessler (LPI) for help with data processing, the LRO teams for collecting and producing high quality data, the USGS team for releasing ISIS routines for processing LRO data, and Matt Weller (Rice University) and Rich Schultz (Univ. of Nevada, Reno) for discussions about fault modeling.